A 202 GHz Link Using Planar Transceiver Modules

Utku Soylu[1], Amirreza Alizadeh[1], Munkyo Seo[2], Ahmed S. H. Ahmed[1], Mark J. W. Rodwell[1]

1 Department of Electrical and Computer Engineering, University of California, Santa Barbara, USA
2 Department of Electrical and Computer Engineering, Sungkyunkwan University, South Korea

***Abstract*— We report a 202 GHz wireless data transmission link, communicating 32 Gb/s over 7.1 meters, using planar InP HBT transmitter and receiver modules. The modules are highly integrated and require simple physical assembly without waveguide interfaces. A single 2.8 mm × 0.75 mm InP HBT transmitter IC and a single 2.3 mm × 0.85 mm InP HBT receiver IC, operating from a 24.5 GHz local oscillator (LO) reference, provide frequency conversion between 6 GHz (I, Q) intermediate-frequency (IF) and the 202 GHz modulated carrier. Signals are radiated and received by directly wire-bonding the InP ICs to 2 × 2 patch antenna arrays on 50 µm SiO_2 substrates, with these antennas coupled to external 50 mm diameter PTFE lenses. 8 Gbaud 16QAM data transmission (32 Gb/s) over 7.1 m, on a link with 10.4 dB added attenuation, showed 13.4% RMS error vector magnitude.**

Keywords—mm-wave wireless, 6G wireless, mm-wave ICs, THz wireless, mm-wave MIMO.

I. Introduction

150-300 GHz wireless backhaul links can provide very high data transmission capacity, both because of the high available bandwidths and because the short wavelengths can support 4-8 channels of spatial multiplexing (MIMO) even with short arrays [1]. There has been extensive development [2] of 150-300 GHz transceiver ICs, modules, and links, including results with InP HBT ICs at 142 GHz [3], SiGe HBT ICs at 135 GHz [4] and 230 GHz [5], and results with InGaAs HEMT ICs at 240 GHz [6, 7, 8] and 300 GHz [9, 10, 11, 12, 13].

Many of the reported transceivers and links, particularly at and above 200 GHz, have used low scales of integration, with the transmitter and receiver assembled from several waveguide modules, each containing a separate IC. 150-300 GHz waveguide modules demand tight dimensional tolerances and are thus expensive to machine. We had earlier reported [14] integrated 200 GHz transmitter and receiver ICs. Here we report 200 GHz transmitter and receiver modules assembled by planar packaging to avoid waveguide interfaces. We demonstrate these modules with short-range data transmission experiments, with signal beam attenuation deliberately added to keep the receiver within its linear dynamic range.

This work was supported in part by the Semiconductor Research Corporation and DARPA under the JUMP program and in part by a contract from Samsung corporation. A portion of this work was performed in the UCSB Nanofabrication Facility, an open access laboratory.

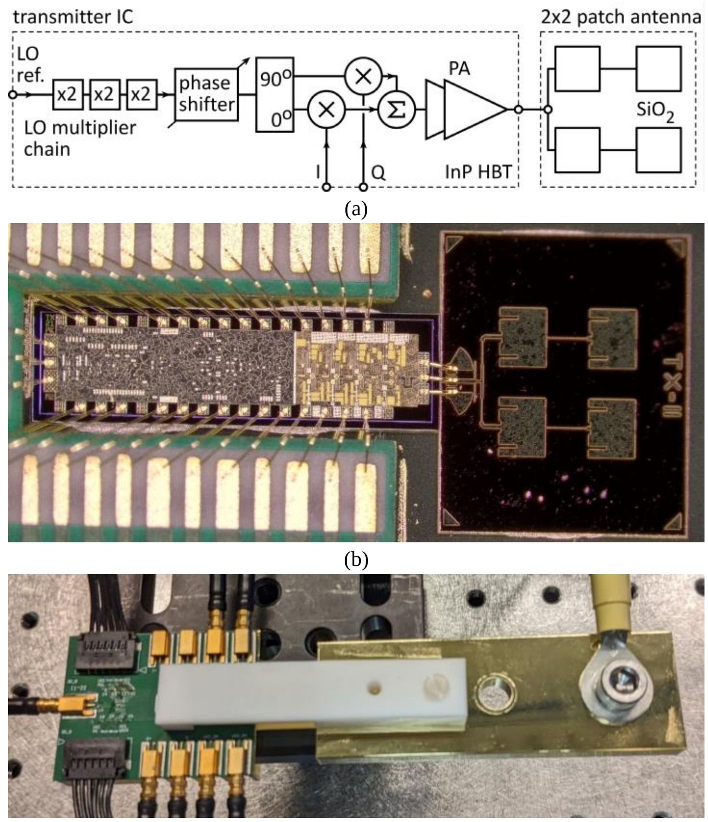

Figure 1. 200 GHz transmitter module: (a) block diagram, (b) photograph showing the InP HBT transmitter IC and the patch antenna array on fused silica, and (c) view of the full module, showing the PCB, connectors, heat sink, and PTFE radome.

II. Transmitter and Receiver Modules

The transmitter (Figure 1) and receiver modules (Figure 2) contain an InP HBT transmitter or receiver IC, a 2 × 2 microstrip patch antenna array on a fused silica (SiO_2) substrate, and a low-frequency printed circuit board (PCB) providing power, LO reference, and (I,Q) interface connections. The IC, PCB, and SiO_2 antenna substrate are bonded, with a high thermal conductivity adhesive, to a (Au, Ni)-plated copper heat sink and support. A PTFE (ε_r =2.1) cover protects the IC and wire bonds from mechanical damage.

The 2.8 mm × 0.75 mm transmitter IC (Figure 1a) contains an 8:1 frequency multiplier, an (I, Q) upconversion mixer, and a power amplifier (PA). The 2.3 mm × 0.85 mm receiver IC (Figure 2a) contains the frequency multiplier, an (I, Q) down conversion mixer, an input low-noise amplifier (LNA) [15],

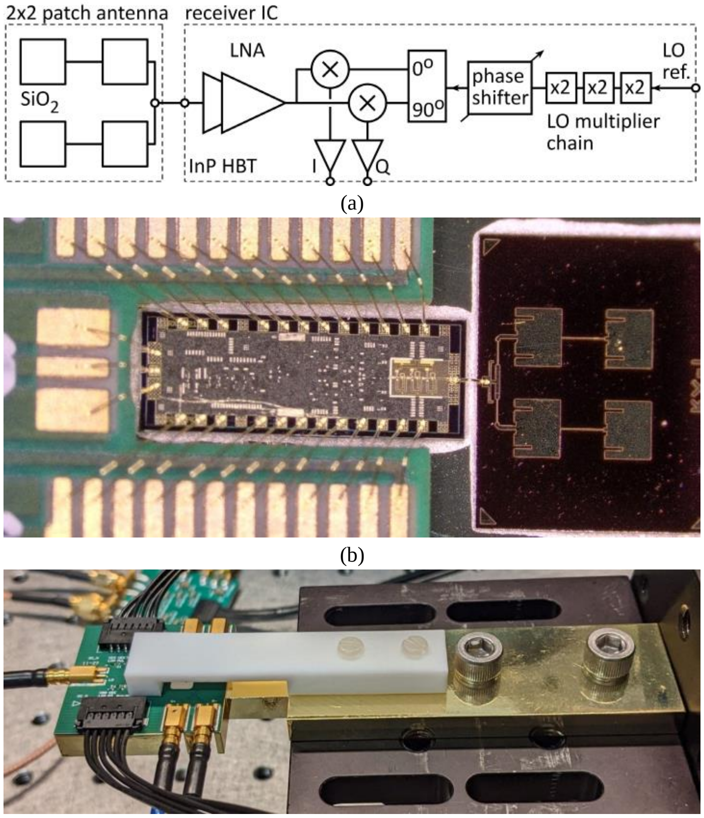

Figure 2. 200 GHz receiver module: (a) block diagram, (b) photograph showing the InP HBT receiver IC and the patch antenna array on fused silica, and (c) view of the full module, showing the PCB, connectors, heat sink, and PTFE radome.

and 50 Ω output amplifiers for the differential (I, Q) outputs. The ICs were fabricated in 250 nm InP HBT technology [16].

The receiver ICs have 24 dB peak conversion gain and ~20 GHz bandwidth (Figure 3a) and 7.7-9.3 dB noise figure over 200-212 GHz (Figure 3b). The transmitter ICs have 34 dB peak conversion gain and > 20 GHz bandwidth (Figure 3c), 16.5 dBm saturated output power at 190 GHz and 15.3 dBm at 200 GHz (Figure 3d); note that the peak power amplifier output power is at a frequency well below 200 GHz.

A wedge-bonder connected the ICs to the antennas using 1 mil diameter Au bond wires. We simulated the full IC-antenna interface, including the antennas, wire bonds, InP through-substrate vias, and even the LNA input matching network and the PA output matching network. Tuning elements added to the SiO_2 antenna substrate compensate for the bond wire parasitics and re-tune the center frequencies of the receiver LNA and transmitter towards the intended 200 GHz frequency of operation. These electromagnetic simulations, and detailed antenna measurements, will be reported separately.

The receiver gain ($P_{out,IF}$/EIRP) is 29 dB, with 194-208 GHz 3-dB bandwidth, while the transmitter gain (EIRP/$P_{in,IF}$), 41.4 dB ± 3.5 dB over 196-218 GHz, has strong frequency-dependent ripple, though this ripple may be a measurement artifact. The transmitter module saturated EIRP is 21.5 dBm at 200 GHz (Figure 4). The transmitter and receiver modules have c.a. 62° beamwidth in both E-plane and H-plane.

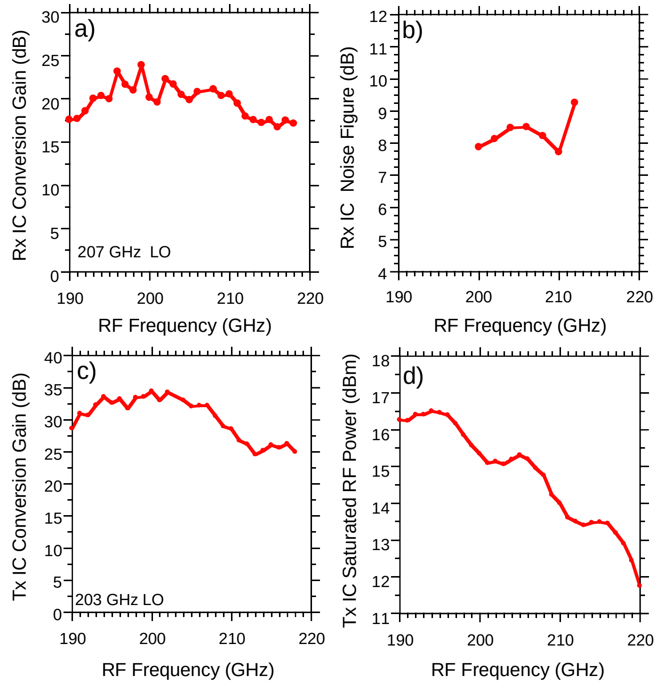

Figure 3. Measured [14] receiver IC conversion gain (a), receiver IC noise figure (b), transmitter IC conversion gain (c), and transmitter IC saturated RF output power (d).

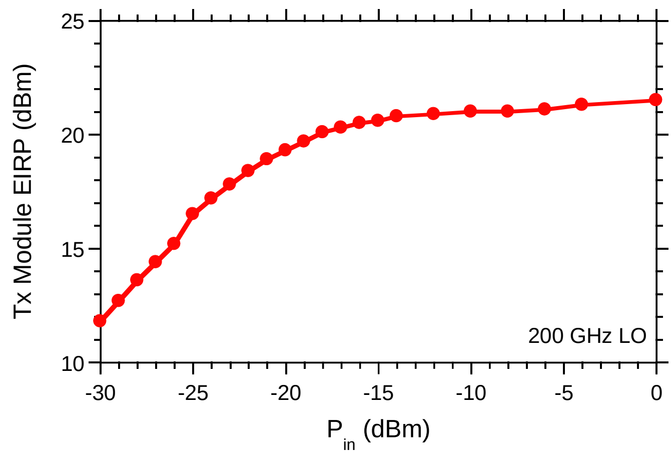

Figure 4. Measured transmitter module EIRP vs. baseband input power.

III. Transmission Experiment

In the transmission experiment (Figure 5), an arbitrary waveform generator (Keysight M8195A) generates an (I, Q) pair of 6 GHz IF signals, these carrying QAM or QPSK modulation. The transmitter LO port is driven with 24.5 GHz, generating a 196 GHz LO. The transmitter then operates as a single-sideband frequency upconverter, producing a 202 GHz modulated carrier. The receiver, also driven with a 24.5 GHz LO reference from the same source, produces a demodulated 6 GHz (I, Q) output. These are summed with a 90° hybrid, and the signal recorded with a digital storage oscilloscope (Keysight DSAV134A). Signal processing algorithms (Keysight VSA2022) provides adaptive equalization with 80 filter taps; the transmitted waveforms are root-raised-cosine with α=0.35.

Table I. Comparison of 140-300 GHz transceivers and link experiments

Ref.	**Frequency** GHz	**Rate** Gb/s	**Range** m	**Modulation**	**Technology**	P_{out} dBm	**Noise** dB	**Transceiver Integration** (WG = waveguide)	**Antenna-IC connection**
[4]	145	36	NA[2]	64QAM	SiGe HBT	13[3]	8.5[4]	ICs in radio-on-glass package; 34-43 GHz LO	radio-on-glass
[5]	230	100	1	16QAM	SiGe HBT	8.5[3]	11[4]	ICs mounted on substrate lens; ~16 GHz LO	antenna-on-IC
[6]	240	40	96	8PSK	InGaAs HEMT	-3.6[5]	6[6]	ICs in WG modules; separate 120 GHz LO WG modules	IC-WG bond
[7]	240	---	---	---	InGaAs HEMT	1[3]	4.8[4]	transmitter, receiver ICs used in [6]	---
[8]	240	64	850	8PSK	InGaAs HEMT	-4.5[5]	11[6]	ICs in WG modules; separate 120 GHz LO WG modules	IC-WG bond
[9]	300	10	1.5	32QAM	InGaAs HEMT	9.5[5]	10[6]	WG modules for RX, TX, power amplifier, 84 GHz LO source	IC-WG bond
[10]	300	100	15	16QAM	InGaAs HEMT	-1.2	8.5[6]	TX = probed photodiode; RX IC in WG module, 100 GHz LO	IC-WG bond
[11]	300	50	1	QPSK	InGaAs HEMT	-7[5]	6.7[6]	ICs in WG modules; separate 100 GHz LO WG modules	IC-WG bond
[12]	300	120	9.8	16QAM	InGaAs HEMT	12[5]	15[6]	4 WG modules for TX; 4 for RX, plus 270 GHz LO sources	IC-WG bond
This work	202	32	7.1	16QAM	InP HBT	15[3]	8.5[4]	Integrated TX & RC ICs; antenna-in-package	IC-antenna bond

[1]DSB noise figure, [2]short waveguide section, [3]P_{sat} of IC, [4]IC noise figure [5]P_{sat} of transmit module, [6]receiver module noise figure.

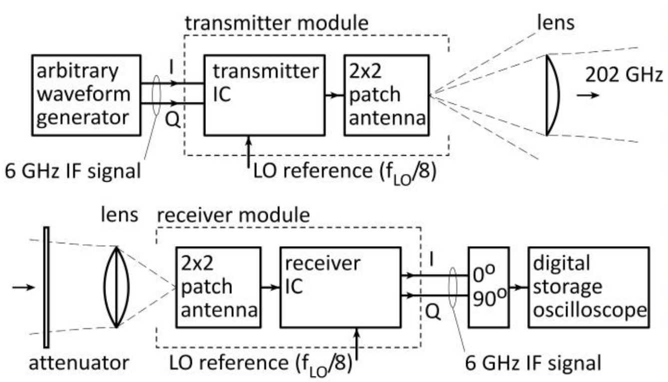

Figure 5. Block diagram of the 202 GHz wireless link. The transmitter is driven by a 6 GHz (I, Q) IF signal carrying QAM or QPSK modulation and radiation from the transmitter patch antenna is partially captured and collimated by a PTFE lens. The receiver, at 7.1 m distance, has a 10.4 dB attenuator and a collimating lens. The receiver 6 GHz (I, Q) IF output is combined by a 90° hybrid and captured by a digital storage oscilloscope.

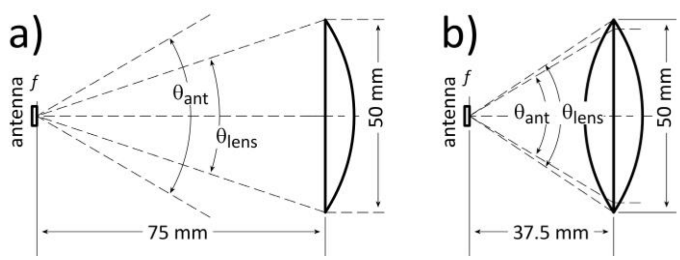

Figure 6. Transmitter and receiver external optics. The transmitter (a) uses a single 50 mm diameter lens whose maximum acceptance angle θ_{lens}=37° is smaller than the antenna 3dB beamwidth θ_{ant}=62°. The receiver (b) uses back-back lenses, increasing θ_{lens} to 68°, larger than the antenna beamwidth.

To provide much larger antenna gains than that of the 2 × 2 patch antennas themselves, the antennas are coupled to external PTFE lenses having 50 mm diameter and 75 mm focal length; an ideal, uniformly illuminated 50 mm diameter aperture has 40.5 dB directivity at 202 GHz. Note that the 62° antenna beamwidth is larger than the 2· arctan (25 mm/ 75 mm) =37° lens maximum acceptance angle (Figure 6a). At the receiver, a pair of back-back PTFE lenses forms a composite lens of 1/2 the focal length, 37.5 mm. The lens acceptance angle is then 68°, and the antenna then couples well to the lens (Figure 6b).

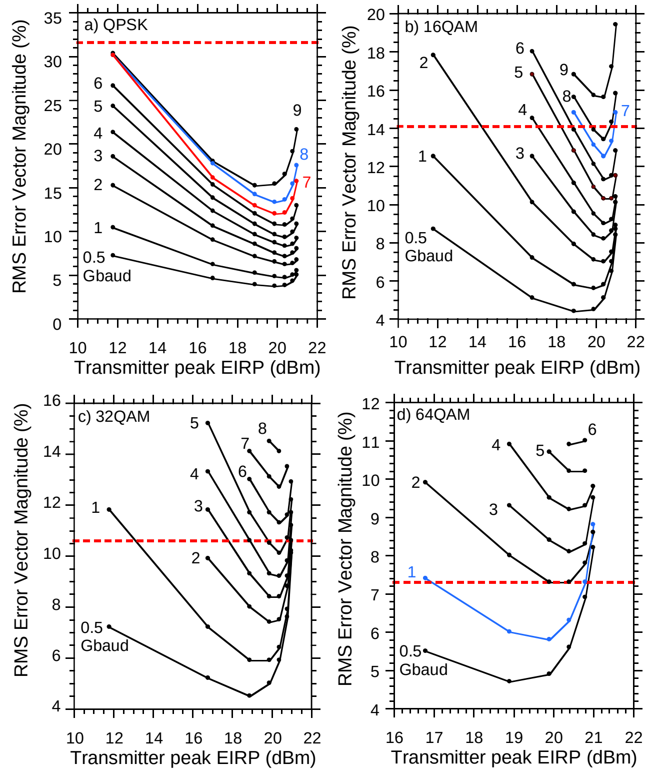

Figure 7. Measured RMS error vector magnitude (EVM), at the receiver, as a function of the transmitter peak EIRP, for (a) QPSK, (b) 16QAM, (c) 32QAM, and (d) 64QAM modulation, with symbol rates varying from 0.5 Gbaud to 9 Gbaud. The red dotted lines indicate the EVM corresponding to 10^{-3} bit error rate for additive white Gaussian noise.

At 7.1 m transmission range, if the lens arrangements of Figure 6a are used at both the transmitter and the receiver, the error vector magnitude at the receiver is observed to increased due to limited receiver dynamic range. To reduce the received power by 4.5 dB, in the 7.1 m link experiments, the lens arrangement of Figure 6a is used for the transmitter while the arrangement of Figure 6b is used for the receiver. To further reduce the received power, a several stacked carboard sheets were placed in the beam path as an attenuator. These provided an additional 10.4 dB attenuation. The total introduced attenuation is 14.9 dB. Without this attenuation, the same link signal/noise ratio would be obtained at $(7.1\text{ m})\cdot 10^{(14.9\text{ dB}/20\text{dB})}$ = 40 meters.

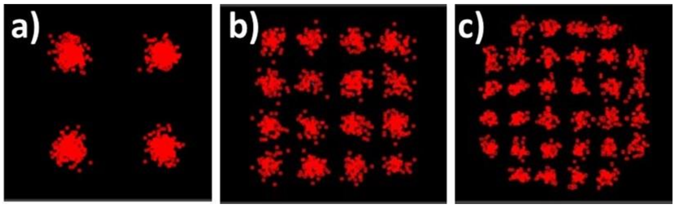

Figure 8. Received data constellations, after adaptive equalization, for (a) 9 Gbaud QPSK (15.1% RMS EVM), (b) 8 Gbaud 16QAM (13.5% RMS EVM), and (c) 5 Gbaud 32QAM (10.1% EVM).

Figure 7 shows the RMS error vector magnitude (EVM) for QPSK (Figure a), 16QAM (Figure b), 32QAM (Figure c), and 64QAM (Figure d) data transmission. The red dotted lines indicate the EVM corresponding to 10^{-3} bit error rate for additive white Gaussian noise. Under these EVM limits, 9 Gbaud (18 Gb/s) transmission is demonstrated for QPSK, 8 Gbaud (32 Gb/s) for 16QAM, 5 Gbaud (25 Gb/s) for 32QAM, and 2 Gbaud (16 Gb/s) for 64QAM. Figure shows measured received data constellations, after adaptive equalization, for 9 Gbaud QPSK (15.1% RMS EVM), 8 Gbaud 16QAM (13.5% RMS EVM), and 5 Gbaud 32QAM (10.1% EVM).

Table 1 compares the present result to published 140-300 GHz transceivers and link experiments. The modules reported here have much higher levels of integration than reported transceiver modules using InGaAs HEMTs. Further, the transmitter output power compares favorably with other technologies.

IV. CONCLUSIONS

We have demonstrated 202 GHz transmitter and receiver modules in 250 nm InP HBT technology. The modules attain higher levels of integration than previously reported 200-300 GHz transceivers using InGaAs HEMTs, attain significantly larger transmitter output power, and avoid the expense of precision machined waveguide packages. Future efforts include small beamsteering phased arrays, for increased range and for less difficult beam alignment, and demonstration of similar modules at 280 GHz.

ACKNOWLEDGMENTS

The authors thank Kyocera for fabrication of the 200 GHz modules. Thanks to Gary Xu and Navneet Sharma of Samsung Research America for guidance and encouragement. Thank so Logan Whitaker, and UCSB cleanroom, Demis D. John, Biljana Stamenic, for antenna process flow development and fabrication.

REFERENCES

[1] M. J. W. Rodwell et al., "IC and Array Technologies for 100-300GHz Wireless," 2022 IEEE Custom Integrated Circuits Conference (CICC), Newport Beach, CA, USA, 2022, pp. 01-05.

[2] T. Maiwald et al., "A Review of Integrated Systems and Components for 6G Wireless Communication in the D-Band," in Proceedings of the IEEE, vol. 111, no. 3, pp. 220-256, March 2023.

[3] S. Carpenter, Z. He, M. Bao and H. Zirath, "A Highly Integrated Chipset for 40 Gbps Wireless D-Band Communication Based on a 250 nm InP DHBT Technology," 2014 IEEE Compound Semiconductor Integrated Circuit Symposium (CSICS), La Jolla, CA, USA, 2014, pp. 1-4.

[4] A. Singh et al., "A D-Band Radio-on-Glass Module for Spectrally-Efficient and Low-Cost Wireless Backhaul," 2020 IEEE Radio Frequency Integrated Circuits Symposium (RFIC), Los Angeles, CA, USA, 2020, pp. 99-102.

[5] P. Rodríguez-Vázquez, J. Grzyb, B. Heinemann and U. R. Pfeiffer, "A 16-QAM 100-Gb/s 1-M Wireless Link With an EVM of 17% at 230 GHz in an SiGe Technology," in IEEE Microwave and Wireless Components Letters, vol. 29, no. 4, pp. 297-299, April 2019.

[6] F. Boes et al., "Ultra-broadband MMIC-based wireless link at 240 GHz enabled by 64GS/s DAC," 2014 39th International Conference on Infrared, Millimeter, and Terahertz waves (IRMMW-THz), Tucson, AZ, USA, 2014, pp. 1-2.

[7] D. Lopez-Diaz et al., "A subharmonic chipset for gigabit communication around 240 GHz," 2012 IEEE/MTT-S International Microwave Symposium Digest, Montreal, QC, Canada, 2012, pp. 1-3.

[8] I. Kallfass, F. Boes, T. Messinger, J. Antes, A. Inam, U. Lewark, A. Tessmann, R. Henneberger 64 Gbit/s Transmission over 850 m Fixed Wireless Link at 240 GHz Carrier Frequency, Journal of Infrared, Millimeter, and Terahertz Waves, Vol. 36, pp 221–233 (2015).

[9] D. Wrana, L. John, B. Schoch, S. Wagner and I. Kallfass, "Short Range Wireless Transmission Using a 295–315 GHz Superheterodyne Link Targeting IEEE802.15.3d Applications," 2021 51st European Microwave Conference (EuMC), London, United Kingdom, 2022, pp. 205-208.

[10] I. Dan et al., "A 300-GHz Wireless Link Employing a Photonic Transmitter and an Active Electronic Receiver With a Transmission Bandwidth of 54 GHz," in IEEE Transactions on Terahertz Science and Technology, vol. 10, no. 3, pp. 271-281, May 2020.

[11] I. Kallfass et al., “Towards MMIC-Based 300 GHz indoor wireless communication systems,” IEICE Trans. Electron., vol. E98-C, no. 12, pp. 1081–1090, Dec. 2015.

[12] H. Hamada et al., "300-GHz-Band 120-Gb/s Wireless Front-End Based on InP-HEMT PAs and Mixers," in IEEE Journal of Solid-State Circuits, vol. 55, no. 9, pp. 2316-2335, Sept. 2020.

[13] C. Castro, R. Elschner, T. Merkle, C. Schubert and R. Freund, "Long-range High-Speed THz-Wireless Transmission in the 300 GHz Band," 2020 Third International Workshop on Mobile Terahertz Systems (IWMTS), Essen, Germany, 2020, pp. 1-4.

[14] M. Seo et al, "A 200 GHz InP HBT Direct-Conversion LO-Phase-Shifted Transmitter/Receiver with 15 dBm Output Power," 2021 IEEE MTT-S International Microwave Symposium (IMS), Atlanta, GA, USA, 2021, pp. 378-381.

[15] U. Soylu, A. S. H. Ahmed, M. Seo, A. Farid and M. Rodwell, "200 GHz Low Noise Amplifiers in 250 nm InP HBT Technology," 2021 16th European Microwave Integrated Circuits Conference (EuMIC), London, United Kingdom, 2022, pp. 129-132.

[16] M. Urteaga, Z. Griffith, M. Seo, J. Hacker and M. J. W. Rodwell, "InP HBT Technologies for THz Integrated Circuits," in Proceedings of the IEEE, vol. 105, no. 6, pp. 1051-1067, June 2017.